# Product Datasheet

## Nrf2 Antibody
## NBP1-32822

Unit Size: 0.1 ml

Aliquot and store at -20C or -80C. Avoid freeze-thaw cycles.

www.novusbio.com technical@novusbio.com

**Reviews: 4 Publications: 67**

Protocols, Publications, Related Products, Reviews, Research Tools and Images at:
www.novusbio.com/NBP1-32822

Updated 12/20/2023 v.20.1



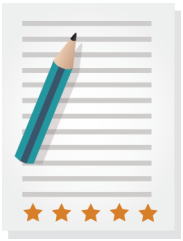

# NBP1-32822

Nrf2 Antibody

| Product Information | |
|---|---|
| **Unit Size** | 0.1 ml |
| **Concentration** | Concentrations vary lot to lot. See vial label for concentration. If unlisted please contact technical services. |
| **Storage** | Aliquot and store at -20C or -80C. Avoid freeze-thaw cycles. |
| **Clonality** | Polyclonal |
| **Preservative** | 0.025% Proclin 300 |
| **Isotype** | IgG |
| **Purity** | Immunogen affinity purified |
| **Buffer** | PBS (pH7), 20% Glycerol |
| **Target Molecular Weight** | 68 kDa |

| Product Description | |
|---|---|
| **Host** | Rabbit |
| **Gene Symbol** | NFE2L2 |
| **Species** | Human, Mouse, Rat, Alligator, Avian, Plant, Zebrafish |
| **Immunogen** | Recombinant protein encompassing a sequence within the center region of human NRF2. The exact sequence is proprietary. |

| Product Application Details | |
|---|---|
| **Applications** | Western Blot, Simple Western, Flow Cytometry, Immunocytochemistry/ Immunofluorescence, Immunohistochemistry, Immunohistochemistry-Paraffin, Immunoprecipitation, Chromatin Immunoprecipitation (ChIP), Knockdown Validated |
| **Recommended Dilutions** | Western Blot 1:500-1:3000, Simple Western -Reported by internal validation, Flow Cytometry -Assay dependent, Immunohistochemistry 1:100-1:1000, Immunocytochemistry/ Immunofluorescence 1:100-1:1000, Immunoprecipitation 1:100-1:500, Immunohistochemistry-Paraffin 1:100-1:1000, Chromatin Immunoprecipitation (ChIP) -Assay dependent, Knockdown Validated |
| **Application Notes** | In Simple Western internal validation: Rat skin wound at 0.5 mg/ml as sample; separated by size; antibody dilution of 1:20 - 1:500; observed molecular weight was 78 kDa; detected by Chemiluminescence. |

## Images

Hydralazine enhances NRF2 signaling in SH-SY5Y cells. c Hydralazine reduced the interaction between NRF2 and KEAP1. Interactions were measured by reciprocal Co-IPs followed by western blot analysis. *p < 0.05, two-tailed Student's t test, n = 3, mean +/- SD. Image collected and cropped by CiteAb from the following publication (http://www.nature.com/articles/s41467-017-02394-3), licensed under a CC-BY license.

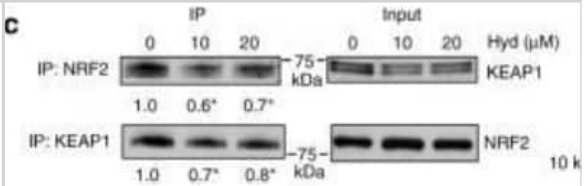

NRF2 antibody [N2C2], Internal detects NRF2 protein at nucleus by immunofluorescent analysis. Sample: HeLa cells were fixed in 4% paraformaldehyde at RT for 15 min. Green: NRF2 stained by NRF2 antibody [N2C2], Internal (NBP1-32822) diluted at 1:500. Red: phalloidin, a cytoskeleton marker, diluted at 1:100.

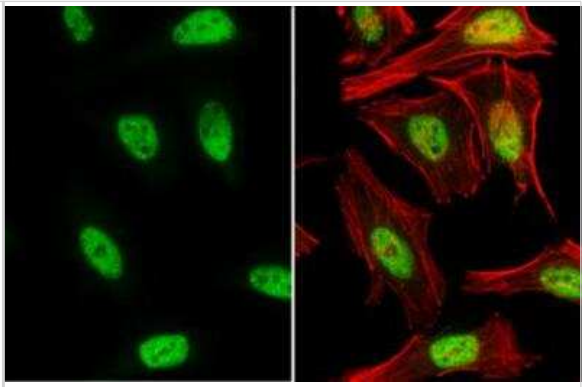

NRF2 antibody [N2C2], Internal detects NRF2 protein at cytoplasm and nucleus by immunohistochemical analysis. Sample: Paraffin-embedded human breast carcinoma. NRF2 stained by NRF2 antibody [N2C2], Internal (NBP1-32822) diluted at 1:500. Antigen Retrieval: Citrate buffer, pH 6.0, 15 min

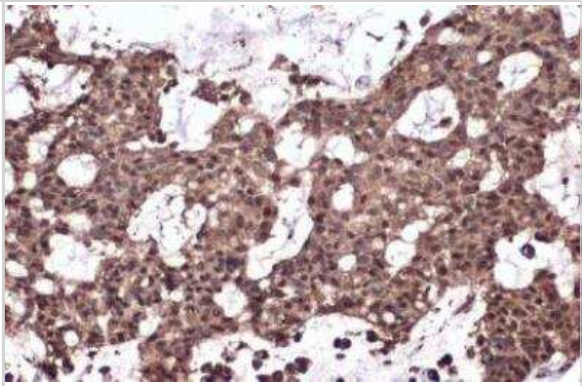

ChIP was performed with HepG2 chromatin extract and 5 ug of either normal rabbit IgG or anti-NRF2 antibody. The precipitated DNA was detected by PCR with primer set targeting to GCLC gene locus.

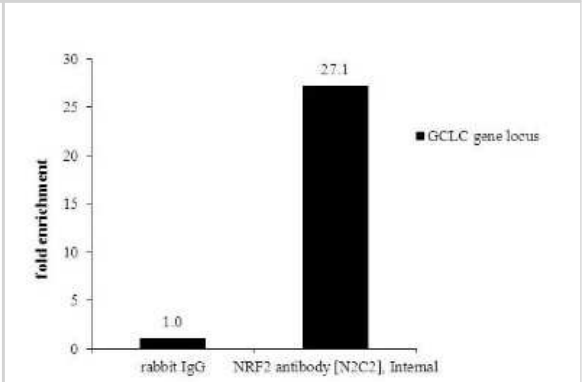


Whole cell extract (30 ug) was separated by 5% SDS-PAGE, and the membrane was blotted with NRF2 antibody [N2C2], Internal diluted at 1:500.

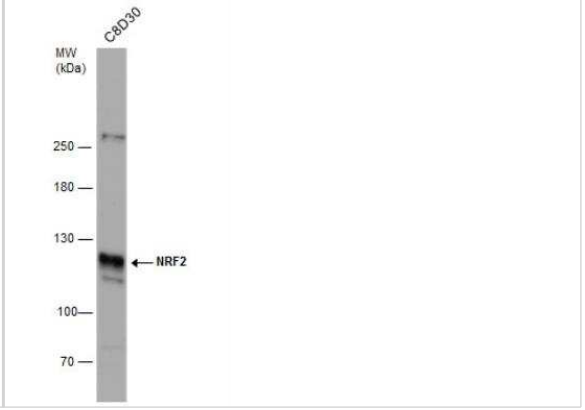

| | |
|---|---|
| Non-transfected (-) and NRF2-transfected (+, including 3xFlag-tag) 293T whole cell extracts (30ug) were separated by 5% SDS-PAGE, and the membrane was blotted with NRF2 antibody diluted by 1:1000. | 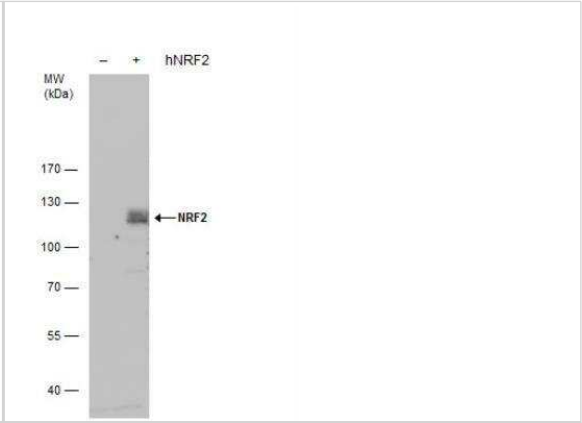 |
| Various whole cell extracts (30 ug) were separated by 7.5% SDS-PAGE, and the membrane was blotted with NRF2 antibody [N2C2], Internal diluted at 1:500. The HRP-conjugated anti-rabbit IgG antibody NBP2-19301) was used to detect the primary antibody, and the signal was developed with Trident ECL plus-Enhanced. | 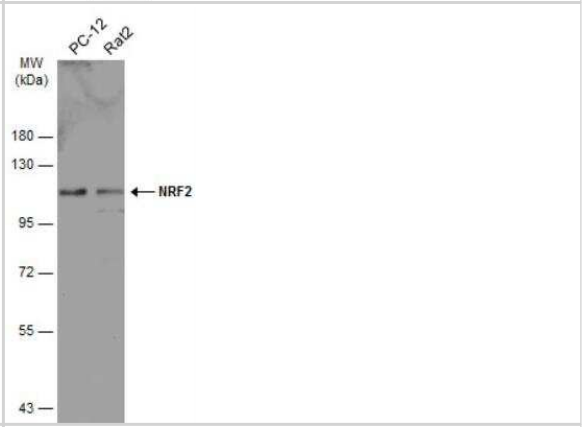 |
| Untreated (-) and treated (+) RAW264.7 whole cell extracts (30 ug) were separated by 5% SDS-PAGE, and the membrane was blotted with NRF2 antibody [N2C2], Internal diluted at 1:500. The HRP-conjugated anti-rabbit IgG antibody (NBP2-19301) was used to detect the primary antibody. | 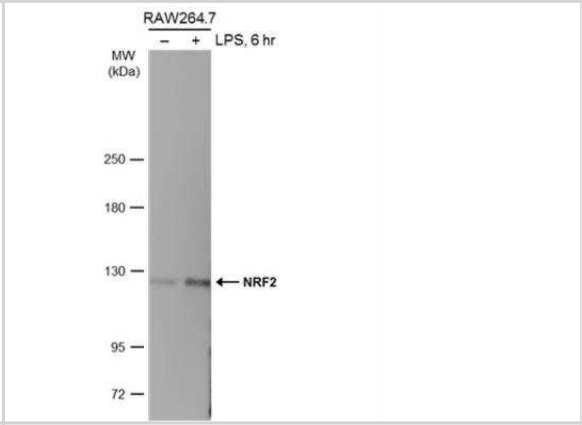 |
| Various whole cell extracts (30 ug) were separated by 7.5% SDS-PAGE, and the membrane was blotted with NRF2 antibody [N2C2], Internal diluted at 1:500. The HRP-conjugated anti-rabbit IgG antibody (NBP2-19301) was used to detect the primary antibody, and the signal was developed with Trident ECL plus-Enhanced. | 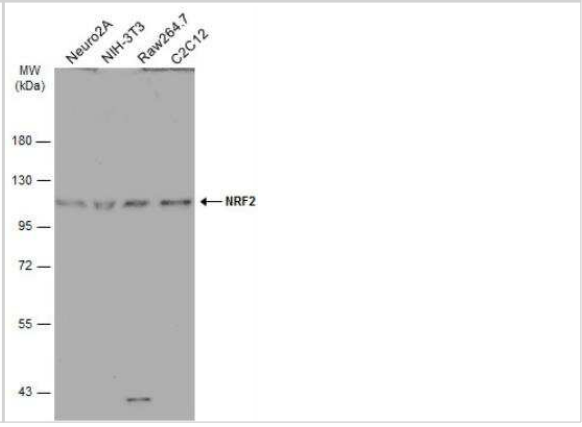 |

| | |
|---|---|
| Untreated (-) and treated (+) Rat-2 whole cell extracts (30 ug) were separated by 5% SDS-PAGE, and the membrane was blotted with NRF2 antibody [N2C2], Internal (NBP1-32822) diluted at 1:500. The HRP-conjugated anti-rabbit IgG antibody (NBP2-19301) was used to detect the primary antibody. | 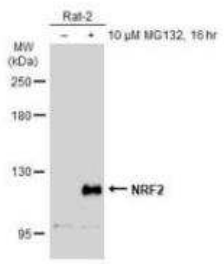 |
| Untreated (-) and treated (+) Neuro2A whole cell extracts (30 ug) were separated by 5% SDS-PAGE, and the membrane was blotted with NRF2 antibody [N2C2], Internal (NBP1-32822) diluted at 1:500. The HRP-conjugated anti-rabbit IgG antibody (NBP2-19301) was used to detect the primary antibody. | 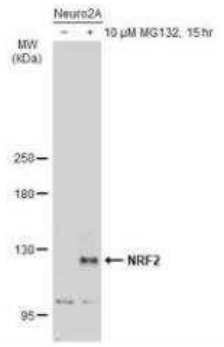 |
| Untreated (-) and treated (+) HepG2 whole cell extracts (30 ug) were separated by 5% SDS-PAGE, and the membrane was blotted with NRF2 antibody [N2C2], Internal (NBP1-32822) diluted at 1:500. The HRP-conjugated anti-rabbit IgG antibody (NBP2-19301) was used to detect the primary antibody. | 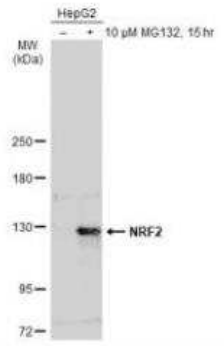 |
| Various whole cell extracts (30 ug) were separated by 5% SDS-PAGE, and the membrane was blotted with NRF2 antibody [N2C2], Internal (NBP1-32822) diluted at 1:500. The HRP-conjugated anti-rabbit IgG antibody (NBP2-19301) was used to detect the primary antibody. | 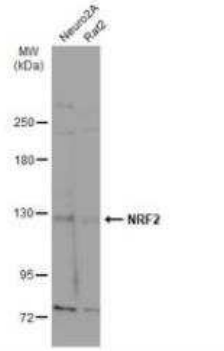 |

| | |
|---|---|
| Untreated (-) and treated (+) MDA-MB-231 nuclear extracts (30 ug) were separated by 7.5% SDS-PAGE, and the membrane was blotted with NRF2 antibody [N2C2], Internal (NBP1-32822) diluted at 1:1000. | 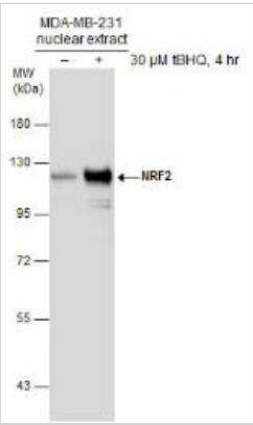 |
| Untreated (-) and treated (+) HepG2 whole cell extracts (30 ug) were separated by 5% SDS-PAGE, and the membranes were blotted with NRF2 antibody [N2C2], Internal (NBP1-32822) diluted at 1:500 and competitor's antibody diluted at 1:500. The HRP-conjugated anti-rabbit IgG antibody (NBP2-19301) was used to detect the primary antibody. | 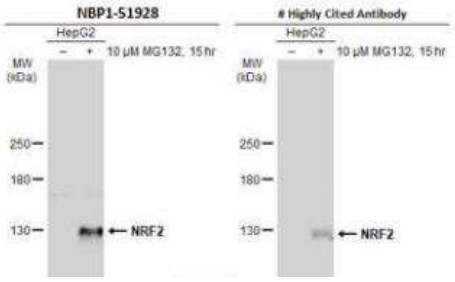 |
| Hydralazine enhances NRF2 signaling in SH-SY5Y cells d NRF2 translocates to the nucleus with hydralazine treatment. Treated cells were subjected to cell fractionation and western blot analysis. *p < 0.05 and **p < 0.01, two-tailed Student's t test, n = 3, mean +/- SD. Image collected and cropped by CiteAb from the following publication (http://www.nature.com/articles/s41467-017-02394-3), licensed under a CC-BY license. | 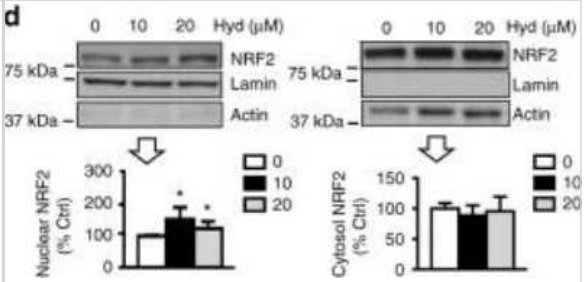 |
| NIH/3T3 cells were fixed in 4% paraformaldehyde at RT for 15 min. Green: NRF2 protein stained by NRF2 antibody [N2C2], Internal diluted at 1:500. Blue: Hoechst 33342 staining. Scale bar = 10 um. | 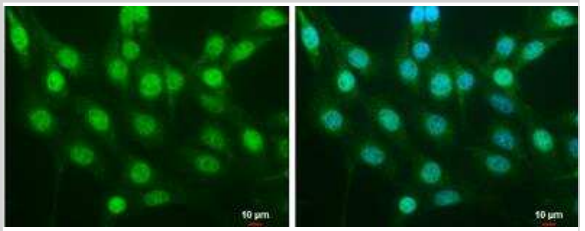 |

| | |
|---|---|
| Immunoprecipitation of NRF2 protein from HepG2 whole cell extracts using 5 ug of NRF2 antibody [N2C2], Internal Western blot analysis was performed using NRF2 antibody [N2C2], Internal.. EasyBlot anti-Rabbit IgG was used as a secondary reagent. | 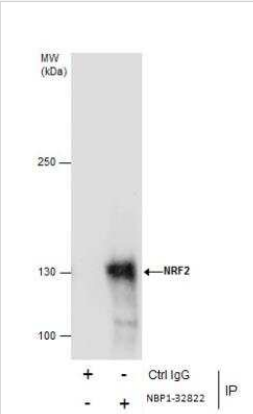 |
| CT activated AMPK/SIRT1 signaling. (A,B) HepG2 cells were treated with 2.5 uM CT for indicated times. Western blot analysis of phosphorylated AMPK, ACC, SIRT1, and Nrf2. Image collected and cropped by CiteAb from the following publication (https://pubmed.ncbi.nlm.nih.gov/31906014), licensed under a CC-BY licence. | 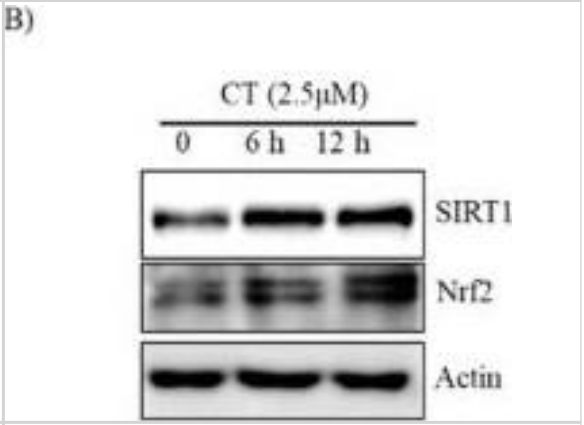 |
| MPE and MSE exert anti-oxidant effects in 3T3-L1 adipocytes. 3T3-L1 cells were treated with pro-differentiative agents for 8 days in the presence or absence of 100 ug/mL MPE or MSE, as reported in Methods. (B) Western blotting analysis of Nrf2, MnSOD and HO-1 in 3T3-L1 cells differentiated without or with 100 ug/mL MPE or MSE. Equal loading of proteins was verified by immunoblotting for beta-actin and showed values were assigned in relation to undifferentiated cells (Undif.). The bar graphs represent the mean of three independent experiments +/- SD. * p < 0.05, ** p < 0.01 with respect to the undifferentiated 3T3-L1 cells, # p < 0.05, ## p < 0.01 and ### p < 0.001 with respect to the differentiated untreated 3T3-L1 cells (Dif.). Image collected and cropped by CiteAb from the following publication (https://pubmed.ncbi.nlm.nih.gov/35204243), licensed under a CC-BY licence. | 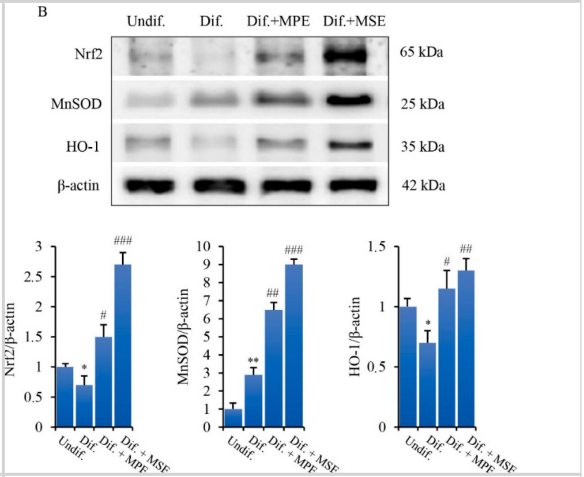 |
| NRF2 modulates epirubicin resistance in breast cancer cells. (C) Expression of NRF2 in MCF-7 cells and MCF-7 EpiR cells was detected by Western blot. beta-Tubulin served as the loading control. (N = 3). Image collected and cropped by CiteAb from the following publication (https://pubmed.ncbi.nlm.nih.gov/32110852), licensed under a CC-BY licence. | 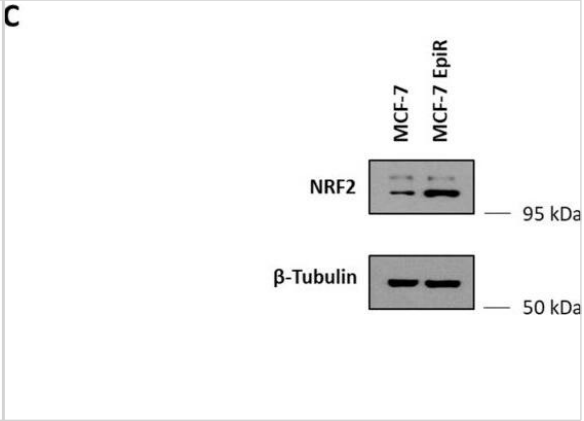 |

Macrophages regulate dormancy in tumor cells.a Representative image of triple immunofluorescently stained in E0771-GFP primary tumor tissue for tumor cells, macrophages, and NR2F1. Green = GFP; Red = NR2F1; White = IBA-1; Blue = DAPI. White arrow shows a macrophage. The yellow arrow shows the contact between an NR2F1-positive tumor cell and a macrophage. Mϕ=Macrophage. Scale bar=20 µm. b Quantification showing the frequency of distances between NR2F1+ tumor cells to the nearest macrophage in the primary tumor. Data is normalized to the frequency of distances between all DAPI+ nuclei to the nearest TMEM. Bar = mean. Error bars = ±SEM. n = 34 fields of view (551 × 316 µm2) in 4 animals. For comparison between the 0 and 200 µm bins a two-tailed Mann-Whitney test was used ($p < 0.0001$). ****$p < 0.0001$. c Representative immunofluorescence images of NR2F1 expression in E0771-GFP tumor cells cultured alone, in direct contact with BAC1.2F5 macrophages, or in direct contact with HUVEC endothelial cells. White arrows show macrophages or endothelial cells in direct contact with a tumor cell. Green = GFP; Red = NR2F1; Blue = DAPI. TC = Tumor Cell. Mϕ = Macrophage. EC = Endothelial Cell. Scale bar = 15 µm. d Percentage of NR2F1-positive tumor cells from each group in C. TC alone: n = 777 cells in 9 independent experiments; TC+Mϕ; n = 226 cells in 6 independent experiments, TC+EC = n = 359 cells in 4 independent experiments. Bar = mean. Error bars = ±SEM. For TC vs. TC+Mϕ ($p = 0.0039$), and for TC vs. TC+EC ($p = 1$), a two-tailed Kruskal-Wallis test with Dunn's multiple comparisons adjustment was used. For TC+Mϕ vs. TC+EC (0.012), a two-tailed one-way ANOVA with Sidak's multiple comparison adjustment was used. *$p < 0.05$. **$p < 0.01$; ns = not significant. Source data are provided as a Source Data file. Image collected and cropped by CiteAb from the following open publication (https://pubmed.ncbi.nlm.nih.gov/35110548), licensed under a CC-BY license. Not internally tested by Novus Biologicals.

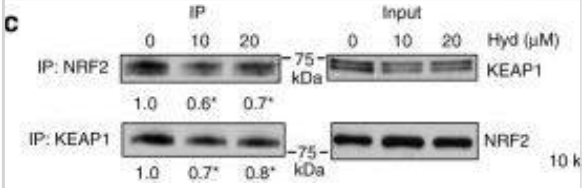


Apoptosis in UV-treated RCC10 cells with mutant VHL proteins correlates to HIF-2α levels. (A) RCC10 cells stably expressing either an empty vector construct (control), wild-type VHLp30 (WT VHL), or various mutant VHLp30 proteins [19] were grown to confluence and lysed. Cell lysates were equally loaded and separated by SDS-PAGE. Western blots were performed for VHL, HIF-2α, and α-tubulin. (B) The RCC10 cell lines in (A) were grown to confluence and treated with UV light and lysed one day later. Cell lysates were equally loaded and separated by SDS-PAGE. Western blots were performed for PARP, cleaved caspase-3, and α-tubulin. (C) Control RCC10 cells and RCC10 cells stably expressing wild-type VHLp30 (WT VHL) were grown to confluence and either left untreated or treated with ultraviolet (UV) light and lysed one day later. Western blots were performed for PARP, cleaved caspase-3, and α-tubulin as in (B). Image collected and cropped by CiteAb from the following open publication (https://cancerci.biomedcentral.com/articles/10.1186/s12935-015-0175-3), licensed under a CC-BY license. Not internally tested by Novus Biologicals.

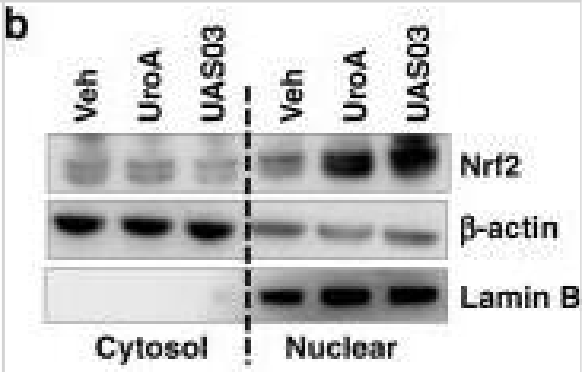

Comparative analysis of reporter gene expression in spermatogonia. a, b Representative whole-mount IF of adult (8–10 weeks post natal) Plzf-mC/CreER; Sox2GFP (a) and Plzf-mC/CreER; Oct4-GFP (b) seminiferous tubules. Inset panels show individual immunostaining within indicated area at higher magnification. Tubule staging and select As and Apr are indicated. Scale bars, 50 μm. c Representative flow cytometry analysis of fixed and permeabilized testis cells from 1 of 3 Oct4-GFP and wild-type (WT) control adults. PLZF+ cell population is shown. Percentages of cells contained within gates are indicated. d Quantification of flow cytometry results from c. Graph indicates percentage of Aundiff (PLZF+ c-KIT−) and cells initiating differentiation (PLZF+ c-KIT+) expressing GFP in Oct4-GFP adults. Horizontal bars indicate mean values (n = 3 mice). e Graph shows percentage of GFRα1+ and SOX3+ spermatogonia positive for GFP in whole-mount seminiferous tubules of Oct4-GFP adults. Spermatogonial identity was confirmed by SALL4 counterstain. Horizontal bars indicate mean values (n = 3 mice, >200 cells scored per data point). f Representative whole-mount IF of adult Oct4-GFP seminiferous tubules for indicated markers (n = 3 mice). Select Aundiff cells are indicated. Scale bar, 50 μm. g Scheme summarizing expression patterns of indicated genes and transgenic reporters plus changes in cell morphology during spermatogonial differentiation. Markers used to isolate different spermatogonial populations are indicated. h Isolation of Oct4-GFP− and Oct4-GFP+ Aundiff from Plzf-mC/CreER; Oct4-GFP adults by flow cytometry. Percentage of cells in each gate from a representative sample is indicated (n = 6 mice). i Oct4-GFP− and GFP+ adult Aundiff fractions were transplanted into recipients and analysed 8 weeks later by whole-mount IF. Images show GFP and mCherry expression in representative colonies. PLZF counterstain confirms Aundiff and spermatogonial identity. Panels show higher magnification details of indicated areas. Scale bar, 100 μm. Graph shows colony-forming efficiency of Oct4-GFP+ and GFP− Aundiff fractions. Data is presented as mean number of colonies per 105 donor cells ± s.e.m. (n = 7 recipient testes for Oct4-GFP− cells and n = 6 for Oct4-GFP+ cells). Donor cells were pooled from 2 Plzf-mC/CreER; Oct4-GFP adults. Significance was calculated by two-tailed Student's t-test (*P < 0.05, ****P < 0.0001) Image collected and cropped by CiteAb from the following open publication (https://www.nature.com/articles/s41467-018-04827-z), licensed under a CC-BY license. Not internally tested by Novus Biologicals.

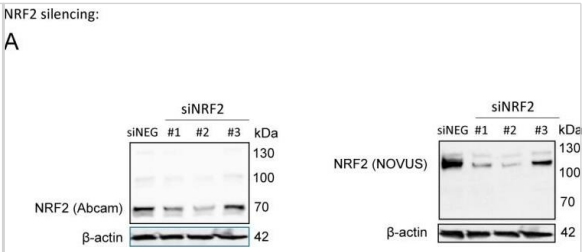


Spy1 stable protein induces anchorage independent growth. (A) 293 cells were transfected with different concentrations of Myc-Spy1-WT, Myc-Spy1-TST or 30 μg of empty PCS3 vector control. Soft agar assay was carried out and plates photographed and quantified on day 14. Foci were averaged over 3 separate transfections for each experiment. n = 3 (B) Western blot analysis of one representative experiment; densitometry in lower panel. n = 3 (C) Representative foci after 14 day soft agar assay visualized using light microscopy. Ras-V12 is transfected as a positive control. n = 3. (D) Total numbers of foci were counted over 3 separate plates using separate transfections for each experiment. n = 3. Error bars reflect SE between triplicate experiments. t test was performed;** P ≤ 0.01. (E) Western blot analysis of experiments in Figure. 1C & D. Quantified using densitometry followed by normalization for Actin levels. (A-E) Error bars reflect SE between triplicate experiments. t test was performed;* P≤ 0.05, ** P ≤ 0.01, *** P ≤ 0.001. Image collected and cropped by CiteAb from the following open publication (https://bmccancer.biomedcentral.com/articles/10.1186/1471-2407-12-45), licensed under a CC-BY license. Not internally tested by Novus Biologicals.

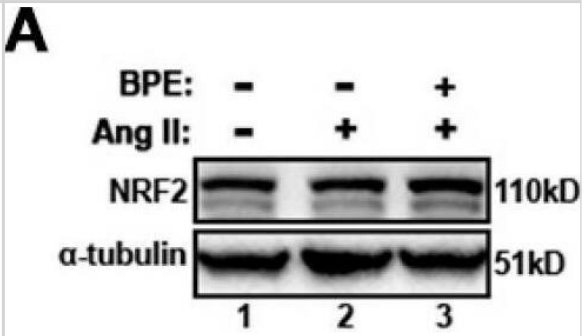

## Publications


Endo M, Tanaka Y, Fukuoka M et al. Wnt5a/Ror2 promotes Nrf2-mediated tissue protective function of astrocytes after brain injury Glia 2023-10-31 [PMID: 37904612]

Madi A, Sheinin R, Salomon K et al. interFLOW: maximum flow framework for the identification of factors mediating the signaling convergence of multiple receptors Research Square 2023-10-31 (IHC, Mouse)

Tabei Y, Abe H, Suzuki S et al. Sedanolide Activates KEAP1-NRF2 Pathway and Ameliorates Hydrogen Peroxide-Induced Apoptotic Cell Death International journal of molecular sciences 2023-11-20 [PMID: 38003720] (Simple Western, Human)

Details:
Dilution 1:50

Moniruzzaman M, Kumar S, Mukherjee M, Chakraborty SB Delineating involvement of MAPK/NF-?B pathway during mitigation of permethrin-induced oxidative damage in fish gills by melatonin Environmental toxicology and pharmacology 2023-11-13 [PMID: 37967690] (WB, Fish)

Annaz H, Abdelaal S, Mandour D et al. Mexican tea (Dysphania ambrosioides (L.) Mosyakin & Clemants) seeds attenuate tourniquet-induced hind limb ischemia-reperfusion injury by modulating ROS and NLRP3 inflammasome pathways Journal of Functional Foods 2023-08-07 (IHC-P, Rat)

El Khoury M, Biondi O, Bruneteau G et al. NADPH oxidase 4 inhibition is a complementary therapeutic strategy for spinal muscular atrophy Frontiers in cellular neuroscience 2023-09-14 [PMID: 37780204] (IHC-Fr, Mouse)

Lane SL, Parks JC, Russ JE et al. Increased Systemic Antioxidant Power Ameliorates the Aging-Related Reduction in Oocyte Competence in Mice International Journal of Molecular Sciences 2021-12-01 [PMID: 34884824] (IHC, IHC-P)

Xie T, Cai J, Yao Y et al. LXA4 protects against blue-light induced retinal degeneration in human A2E-laden RPE cells and Balb-c mice Annals of Translational Medicine 2021-08-01 [PMID: 34532386] (WB, IP)

Di Lollo V, Canciello A, Peserico A et al. Unveiling the immunomodulatory shift: Epithelial-mesenchymal transition Alters immune mechanisms of amniotic epithelial cells iScience 2023-09-15 [PMID: 37680464] (B/N)

Zhang W, Xiao D, Li X et al. SIRT1 inactivation switches reactive astrocytes to an antiinflammatory phenotype in CNS autoimmunity Journal of Clinical Investigation 2022-11-15 [PMID: 36136587]

K?l?□ GA, Alsafi M. ?-Glucan Regulates Lipopolysaccharide Induced Genotoxic Damage to The Liver through The Induction of BRCA1 Protein Expression Cell J 2023-09-09 [PMID: 37718767] (ICC/IF)

Hussein MM, Sayed RKA, Mokhtar DM. Structural and immunohistochemical analysis of the cellular compositions of the liver of molly fish (Poecilia sphenops), focusing on its immune role Zoological Letters 2023-01-05 [PMID: 36604695] (IHC, EM)


More publications at http://www.novusbio.com/NBP1-32822

**Novus Biologicals USA**
10730 E. Briarwood Avenue
Centennial, CO 80112
USA
Phone: 303.730.1950
Toll Free: 1.888.506.6887
Fax: 303.730.1966
nb-customerservice@bio-techne.com

**Bio-Techne Canada**
21 Canmotor Ave
Toronto, ON M8Z 4E6
Canada
Phone: 905.827.6400
Toll Free: 855.668.8722
Fax: 905.827.6402
canada.inquires@bio-techne.com

**Bio-Techne Ltd**
19 Barton Lane
Abingdon Science Park
Abingdon, OX14 3NB, United Kingdom
Phone: (44) (0) 1235 529449
Free Phone: 0800 37 34 15
Fax: (44) (0) 1235 533420
info.EMEA@bio-techne.com

**General Contact Information**
www.novusbio.com
Technical Support: nb-technical@bio-techne.com
Orders: nb-customerservice@bio-techne.com
General: novus@novusbio.com

## Products Related to NBP1-32822

| | |
|---|---|
| HAF008 | Goat anti-Rabbit IgG Secondary Antibody [HRP] |
| NB7160 | Goat anti-Rabbit IgG (H+L) Secondary Antibody [HRP] |
| NBP2-24891 | Rabbit IgG Isotype Control |
| H00004780-P01-10ug | Recombinant Human Nrf2 GST (N-Term) Protein |

**Limitations**
This product is for research use only and is not approved for use in humans or in clinical diagnosis. Primary Antibodies are guaranteed for 1 year from date of receipt.

**For more information on our 100% guarantee, please visit www.novusbio.com/guarantee**

**Earn gift cards/discounts by submitting a review: www.novusbio.com/reviews/submit/NBP1-32822**

**Earn gift cards/discounts by submitting a publication using this product: www.novusbio.com/publications**